

Generation of analytical redundancy relations for fault detection and isolation of ultrasonic linear motor

Badoud Abd Essalam and Khemliche Mabrouk

Automatic laboratory, Electrical engineering department, University of Setif, Algeria, 19000

Abstract

In this paper Bond Graph modeling, simulation and monitoring of ultrasonic linear motors are presented. Only the vibration of piezoelectric ceramics and stator will be taken into account. Contact problems between stator and rotor (slider) are not treated here. So, standing and travelling waves will be briefly presented since the majority of the motors use another wave type to generate the stator vibration and thus obtain the elliptic trajectory of the points on the surface of the stator in the first time. Then, electric equivalent circuit will be presented with the aim for giving a general idea of another way of graphical modeling of the vibrator introduced and developed. The simulations of an ultrasonic linear motor are then performed and experimental results on a prototype built at the laboratory are presented. Finally, validation of the Bond Graph method for modeling is carried out, comparing both simulation and experiment results. This paper describes the application of the FDI approach to an electrical system. We demonstrate the FDI effectiveness with real data collected from our automotive test. We introduce the analysis of the problem involved in the faults localization in this process. We propose a method of fault detection applied to the diagnosis and to determine the gravity of a detected fault. We show the possibilities of application of the new approaches to the complex system control.

Keywords: Modeling; Monitoring; Ultrasonic Linear Motor; Detection; Isolation; Bond Graph.

1. Introduction

The modeling constitutes an aspect of great importance within all engineering fields because it allows us to understand the behavior of the system without having to experiment on it. It also allows the determination of certain characteristics of the system and can give important information on operating conditions with the use of relatively simple and inexpensive procedures. Moreover, it is an essential tool for the design of fault detection and isolation strategies and very important at industrial level [1].

This instructs Piezoelectric ultrasonic motors, whose efficiency is insensitive to size, are frequently used in the mm-size motor area. In general, piezoelectric motors are classified into two categories, based on the type of driving voltage applied to the device and the nature of the strain induced by the voltage: rigid displacement devices for which the strain is induced unidirectional along an applied DC field, and resonating displacement devices for which the alternating strain is excited by an AC field at the mechanical resonance frequency. The first category can be further divided into two types: servo displacement transducers and pulse-drive motors [2], [3], [4].

The AC resonant displacement is not directly proportional to the applied voltage, but is dependent on the adjustment of the drive frequency. Very high speed motion due to the high frequency is also an attractive feature of the ultrasonic motors. The materials requirements for these classes of devices are somewhat different and certain compounds will be better suited for particular applications. The ultrasonic motor, for instance, requires a very hard piezoelectric with a high mechanical quality factor Q_m , in order to minimize heat generation and maximize displacement. The servo displacement transducer suffers most from strain hysteresis [5].

The pulse-drive motor requires a low-permittivity material rather than a small hysteresis, so that soft PZT materials are preferred. This thesis deals with ultrasonic motors using resonant vibrations. However, after a brief historical background review, different ultrasonic motors are introduced. Working principles and motor characteristics are explained [6].

Fault detection and isolation in complex dynamic systems requires the use of modeling approaches that capture system dynamics and the transients that arise when faults occur. In previous work [7], we have developed a systematic approach using bond graph modeling to derive the temporal causal graph representing the functional relations of a system subject to FDI. The

inherent physical constraints of a bond graph model (conservation of energy, conservation of the physical state, continuity of power) result in well constrained models that prevent the generation of spurious results, one of the most important drawbacks of traditional qualitative methods used in artificial intelligence approaches to the diagnosis problem. The generation of the bond graph modeling approach allows seamless integration of multi domain models (electrical, mechanical and hydraulic) into one representation.

In this paper we show how the qualitative approach to FDI, embodied by the Transcend system applies to the fault isolation in ultrasonic linear motor. To this end, a Bond Graph model of the system is designed that includes mechanical, thermal, and hydraulic phenomena.

2. Bond Graph approach

The Bond Graphs are an independent graphical description of dynamic behavior of the physical systems. This means that the multi domains systems (electrical, mechanical, hydraulic, acoustical, thermodynamic and material) are described in the same way.

The Bond Graphs are based on energy exchange [8]. Analogies between domains are more than just equations being analogous; the used physical concepts are analogous. Bond Graph is a powerful tool for modeling systems, especially when different physical domains are involved [9].

The major advantages of Bond Graph modeling are that in such modeling a topological structure is used to represent the power/energy characteristics of engineering systems, and the systems with different energy domains are treated in a unified manner. A topological representation, such as a Bond Graph, offers great advantage at the conceptual design level, since quantitative details are not required prematurely. In addition, the graphical representations of the complex models are easy and clear. They are the easiest way for a engineers group to communicate the description of energy flows in dynamic systems [1].

Since a Bond Graph is an unambiguous representation of an energy system, it is possible for a computer program to automatically generate the equations for dynamic analysis of the system. The bonds in Bond Graphs model represent the power coupling, such models apply to mechanical translation and rotation, electrical circuits, thermal, hydraulic, magnetic, chemical, and other physical domains. They are especially useful in systems which function in coupled domains, such as electromechanical systems [8].

3. Mechanism of ultrasonic motor

Dry friction is often used in contact, and the ultrasonic vibration induced in the stator is used both to impart motion to the rotor and to modulate the frictional forces present at the interface. The friction modulation allows bulk motion of the rotor; without this modulation, ultrasonic motors would fail to operate.

Two different ways are generally available to control the friction along the stator-rotor contact interface, traveling-wave vibration and standing-wave vibration. Some of the earliest versions of practical motors in the 1970s, for example, used standing-wave vibration in combination with fins placed at an angle to the contact surface to form a motor, albeit one that rotated in a single direction. Later designs by Sashida and researchers at Matsushita, ALPS, and Canon made use of traveling-wave vibration to obtain bi-directional motion, and found that this arrangement offered better efficiency and less contact interface wear.

An exceptionally high-torque 'hybrid transducer' ultrasonic motor uses circumferentially-poled and axially-poled piezoelectric elements together to combine axial and torsional vibration along the contact interface, representing a driving technique that lies somewhere between the standing and traveling-wave driving methods.

A key observation in the study of ultrasonic motors is that the peak vibration that may be induced in structures occurs at a relatively constant vibration velocity regardless of frequency. The vibration velocity is simply the time derivative of the vibration displacement in a structure, and is not related to the speed of the wave propagation within a structure. Many engineering materials suitable for vibration permit a peak vibration velocity of around 1 m/s. At low frequencies 50 Hz, indicate a vibration velocity of 1 m/s in a woofer would give displacements of about 10 mm, which is visible to the eye. As the frequency is increased, the displacement decreases, and the acceleration increases. As the vibration becomes inaudible at 20 kHz or so, the vibration displacements are in the tens of micrometers, and motors have been built that operate using 50 MHz surface acoustic wave (SAW) that have vibrations of only a few nanometers in magnitude. Such devices require care in construction to meet the necessary precision to make use of these motions within the stator.

More generally, there are two types of motors, contact and non-contact, the latter of which is rare and requires a working fluid to transmit the ultrasonic vibrations of the stator toward the rotor. Most versions use air, such as some of the earliest versions by Dr. Hu Junhui. Research in this area continues, particularly in near-field acoustic levitation for this sort of application. (This is different from far-field acoustic levitation, which suspends the

object at half to several wavelengths away from the vibrating object.) [4].

Canon was one of the pioneers of the ultrasonic motor, and made the "USM" famous in the 1980s by incorporating it into its autofocus lenses for the Canon EF lens mount. Numerous patents on ultrasonic motors have been filed by Canon, its chief lens making rival Nikon, and other industrial concerns since the early 1980s. The ultrasonic motor is now used in many consumer and office electronics requiring precision rotations over long periods of time.

4. Description of an annular travelling wave piezomotor

Generally, ultrasonic piezoelectric motors can be designed to use either traveling waves or standing waves to generate motion. Piezoelectric standing wave motors use a combination of flexural, torsional or longitudinal vibrations of a piezoelectric actuator. One vibration produces a normal force while the other generates motion that is perpendicular to the normal force. This combination creates a friction based driving force between one stationary component, the vibrator and the object moved the slider. On the other hand, in a piezoelectric traveling wave motor, traveling waves are generated and propagate in both directions.

Such waves can be classified into two general types. The first type is known as Rayleigh wave [10]. An analogy to this kind of wave is the earth quakes.

The other type of wave known as flexural wave ([11] and [12]) propagates with a snake-like motion. For both Rayleigh and flexural waves, a point of the surface will move following an elliptical trajectory. It is this elliptical motion that provides the drive in traveling wave motors. In the following sections, these two wave types are described more in details.

4.1. Geometry and operation

The operation principle is described on figure 1. This motor is made of two main parts:



Fig. 1. Exploded view of an annular travelling wave motor

The stator: It is a beryllium-copper annular plate. At his circumference, teeth are machined to amplify the vibration movement and eliminate the wear particles. At its bottom surface, piezoelectric ceramics are glued to excite the metallic part. The stator is fixed to the frame at its centre. To guarantee the free vibration of the stator ring, a decoupling fold is machined between the centre and the circumference.

The rotor: It can be separated in 3 zones:

1. The axis, output of the motor;
2. The track friction in contact with the stator;
3. The spring fold linking axis to track and giving the elasticity needed to apply rotor on stator.

Stator/rotor interface: The model of the interface stator-rotor is the most complex part in the ultrasonic motor model. It is supposed that the stator is rigid and its vibration profile does not change after the contact with the rotor, knowing that this one has a conform layer of contact. This part is the one where the interne functional behavior is assured by the existence of some forces. These forces depend on comparison between the displacements speeds of the stator and the rotor respectively [13].

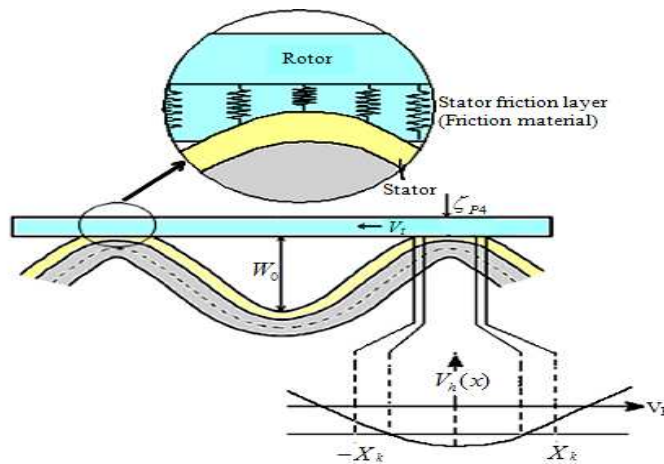


Fig.2. Overlapping between the stator surface and the contact layer of the rotor

One of manners to describe the mechanics of contact is to employ the model of contact zone showed in figure 2. This model supposes that the stator is rigid and the rotor has a contact layer specified as a linear spring with an equivalent rigidity in the axial and tangential direction.

5. Electric equivalent circuit

Depicted in Figure 3, rL is a function of the load torque and applied pre-load pressure. This resistor will model the vibration taking place during the actuation of the motor. It will also take into account of the mechanical and viscous losses in the bearing and other related parts of the ultrasonic motor. [3] Due to the complexity of the interaction between the stator and the rotor, the value of rL has yet to be established. In our case, it will be derived experimentally to establish their relationship.

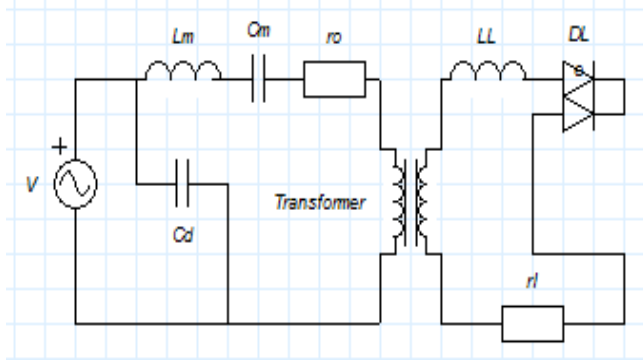


Fig.3. Single phase equivalent circuit for motor

The blocking capacitance Cd lowers the power factor. It would have no effect on the motor's efficiency if there were no line resistance connected between the power supply and the motor. However, under actual operating condition, a lower power factor adversely affects the efficiency, owing to the power source's high internal resistance. To improve the power factor, we can place an inductor in parallel to Cd as shown in Figure 4.

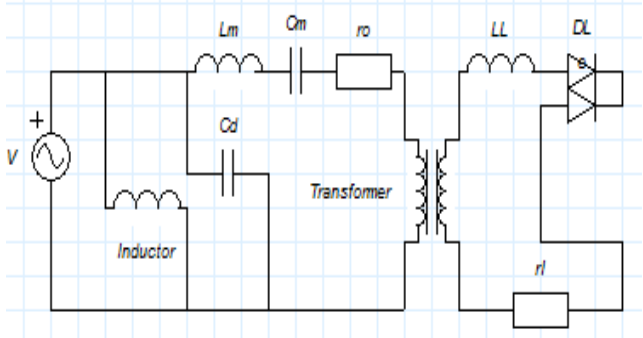


Fig.4. Canceling the effect of blocking capacitance

If Cd is completely cancelled by the inductor, we can then use the simplified equivalent circuit in Figure 5.

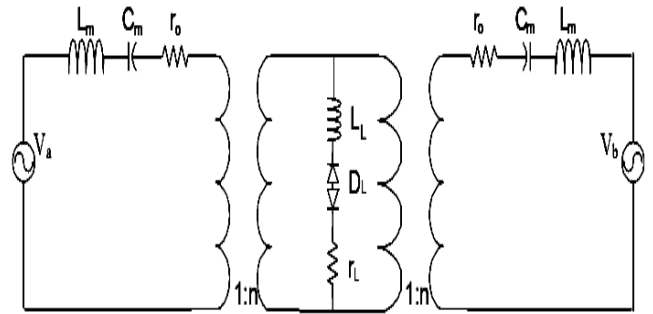


Fig.5. Electric equivalent circuit for the complete motor

Although one may find the physical significance and relationship of the electrical elements in the equivalent circuit easy to understand, its computational analysis is tedious because the diode is a non-linear element [6]. The different components of the electric equivalent circuit are now described and defined.

The value of the static capacitance is given by [14]:

$$C_0 = \epsilon_0 \epsilon_r \frac{S_{el}}{d_{el}} \tag{1}$$

Where ϵ_0 is the free space permittivity, ϵ_r the relative permittivity, S_{el} the surface of the electrodes of the piezoelectric ceramic and d_{el} the distance between the electrodes.

The dielectric resistance R_0 which is in parallel with the static capacitance represents the dielectric losses. For a given frequency, it is given by [12]:

$$R_0 = \frac{1}{\omega C_0 \tan \delta} \tag{2}$$

Where ω is the angular frequency of the considered frequency and $\tan \delta$ is the dielectric dissipation factor.

The motion resistance R_m represents the mechanical losses of the vibrator.

It also includes the losses by friction in the air, the losses due to the glue between the ceramic and the stator. The losses caused by the welding of the connection wires as well as the losses in the electrodes.

C_m and L_m represent the rigidity and the inertia of the vibrator, respectively. They are given by [15]:

$$C_m = \frac{A^2}{K} \tag{3}$$

$$L_m = \frac{m_v}{A^2}$$

Where K is a spring constant and m_v the mass of the vibrator, linked by the following relation:

$$\omega_r = \sqrt{\frac{A}{m_v}} \tag{4}$$

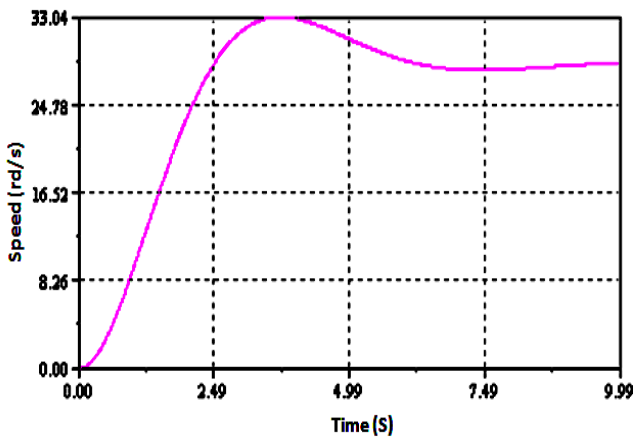


Fig.7. The motor speed without load

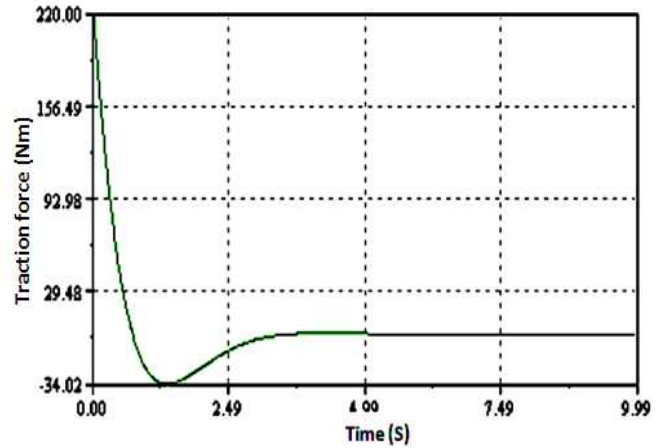


Fig.10. Evolution of traction force a function of time for a load of 300N

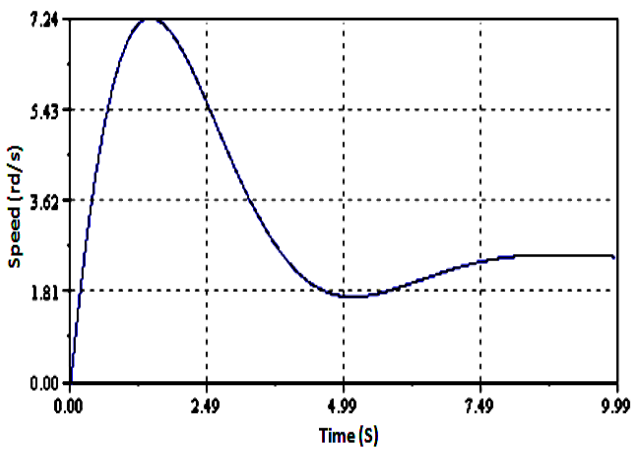


Fig.8. Motor speed as a function of time for a load of 2N

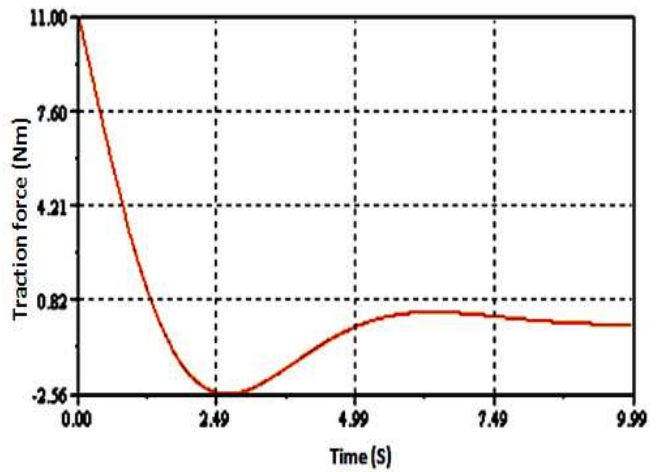


Fig.11. Evolution of traction force a function of time for a load of 3N

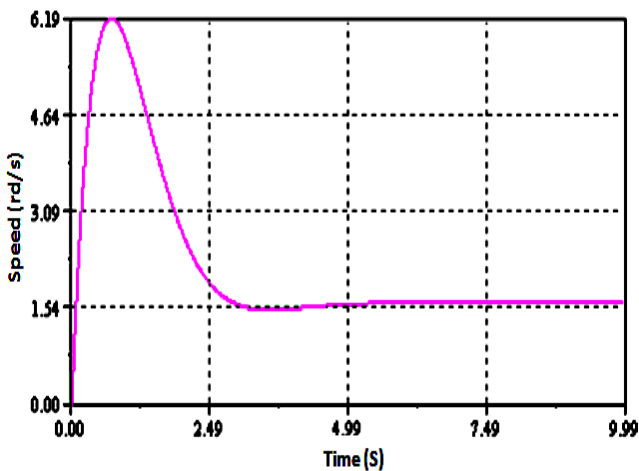


Fig.9. Motor speed as a function of time for a load of 3N

The figure 8 represents the motor speed without load. Figures 9 and 11 shows the evolution of the rotation speed as a function of different loads applied.

Figure 11 and 12 represent respectively the evolution of traction force as functions of time, simulated of different loads applied.

7. Fault Detection and Isolation (FDI)

A number of methods have been developed for fault detection and isolation. All methods of fault detection work by designing residual functions. The residual represents the difference between an estimated value and a measured one, which should be zero during normal operation, but large in the presence of faults [16].

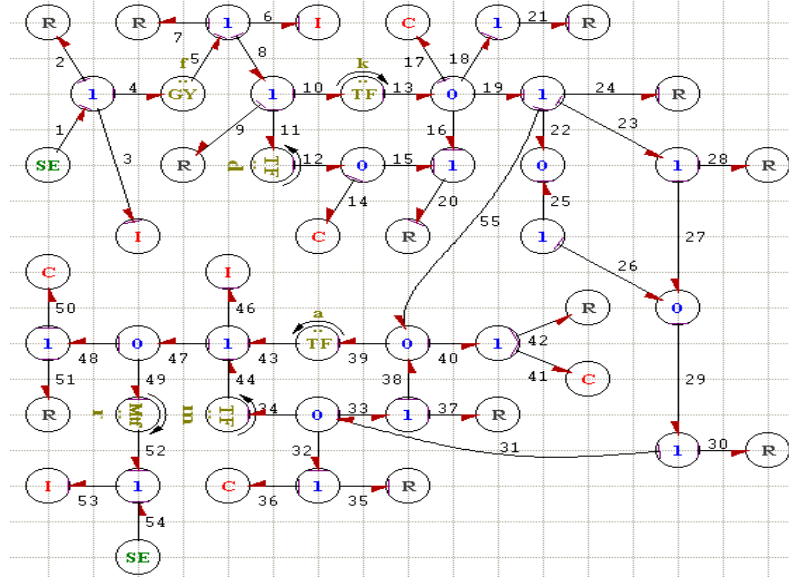


Fig.12. Bond Graph model.

In practice, there is a distinction between the detection of fast-acting, possibly safety-critical faults, and faults which are non-safety-critical and slower to develop, for example due to wear. The former are most likely to be detected by state-estimation and instantaneous comparison of prediction with measurement, while the latter are detected using parameter estimation techniques which require a certain time window and excitation of the system.

Probability analysis can be used to judge, from the residual values, when a fault or change has taken place. This paper is concerned primarily with detection of fast-acting faults, detected via state estimation.

Isolation, in the literature, means diagnosis of the faulty component. If faults are allowed to occur simultaneously, then for a diagnosis, at least as many independent residual functions as faults considered are required. In practice, it is usually assumed that only one fault occurs at a time, which facilitates more robust fault diagnosis [6].

We suppose that sensors and sources are not affected by faults [16].

$$ARR_1 : Se_1 - De_1 - \phi_{I_1} [(1 - y_1)f_3 + y_1 Df_1] - De_2 = 0$$

$$ARR_2 : f(1 - y_1)\Phi_{I_1}(e_3)_1 + \Phi_{I_1} [(1 - y_2)f_6 + y_2 Df_2] - De_3 - De_4 + y_1 Df = 0$$

$$ARR_3 : \frac{1}{S}(1 - x_1)\Phi_{C_1}^{-1}(f_{14}) + \frac{1}{S}(1 - x_2)\Phi_{C_2}^{-1}(f_{17}) + x_2 De_2 - \Phi_{R_4} [(1 - y_3)f_{20} + y_3 Df_3] + x_1 De_1 = 0$$

$$ARR_4 : -\Phi_{R_5} [(1 - y_4)f_{21} + y_4 Df_4] + \frac{1}{S}(1 - x_2)\Phi_{C_2}^{-1}(f_{17}) + x_2 De_2 = 0$$

For our application, the equations in junctions are given by:

For Ii junction:

$$\begin{cases} f_3 = f_1, f_3 = f_2 \\ e_1 - e_2 - e_3 - e_4 = 0 \\ e_{I_1} = \phi_{I_1} [(1 - y_1)f_3 + y_1 Df_1] \\ f_{I_1} = (1 - y_1)\phi_{I_1}(e_3) + y_1 Df_1 \end{cases} \quad (9)$$

For Oj junction:

$$\begin{cases} e_{14} = e_{12}, e_{14} = e_{15} \\ f_{12} - f_{14} - f_{15} = 0 \\ f_{C_1} = \phi_{C_1} [S\{(1 - x_1)e_{14} + x_1 De_1\}] \\ e_{C_1} = \frac{1}{S}(1 - x_1)\phi_{C_1}^{-1}f_{14} + x_1 De_1 \end{cases} \quad (10)$$

From equations of junctions we generate the following ARR:

(11)

$$ARR_5 : x_2 De_2 - \Phi_{R_6} [(1 - y_5) f_{24} + y_5 Df_5] - De_5 + \frac{1}{S} (1 - x_2) \Phi_C^{-1} (f_{17}) + = 0$$

$$ARR_6 : De_7 - \phi_{r_2} [(1 - y_6) f_{35} + y_6 Df_6] - De_8 = 0$$

$$ARR_7 : \frac{1}{m} De_7 + Se_{45} - \Phi_{I_3} [(1 - y_7) f_{46} + y_7 Df_7] - De_{10} + De_9 = 0$$

$$ARR_8 : De_{11} + Se_{54} - \Phi_{I_4} [(1 - y_8) f_{53} + y_8 Df_8] = 0$$

$$ARR_9 : Df_2 - y_3 Df_3 - \Phi_{C_1} [S \{ (1 - x_1) e_{14} + x_1 De_1 \}] - (1 - y_3) \Phi_{R_4} (e_{20}) = 0$$

$$ARR_{10} : Df_1 - \Phi_{C_2} [S \{ (1 - x_2) e_{17} + x_2 De_2 \}] - y_3 Df_3 - (1 - y_4) \Phi_{R_5} (e_{21}) - y_4 Df_4 - (1 - y_3) \Phi_{R_4} (e_{20}) = 0$$

The Bond Graph model of the process is represented by Fig.2.

From the binary variables xi and yj we can determine the final structure of the monitorable system [2]. Two 10-sensor placement combinations provide the monitorability of the all components. The question arises whether we are able to supervise this system by only 9 sensors? And what are the combinations which provide this result?

$$\text{For } : [y_1 y_2 y_3 y_4 y_5 y_6 y_7 y_8 x_1 x_2] = [0111111111]$$

Table 1

Fault signature

| | I1 | I2 | R4 | R5 | R6 | r2 | I3 | I4 | C1 | C2 |
|------|----|----|----|----|----|----|----|----|----|----|
| ARR1 | 1 | 1 | 0 | 0 | 0 | 0 | 0 | 0 | 0 | 0 |
| ARR2 | 0 | 0 | 1 | 0 | 0 | 0 | 0 | 0 | 0 | 0 |
| ARR3 | 0 | 0 | 0 | 1 | 0 | 0 | 0 | 0 | 0 | 1 |
| ARR4 | 0 | 0 | 0 | 0 | 1 | 0 | 0 | 0 | 0 | 1 |
| ARR5 | 0 | 0 | 0 | 0 | 0 | 1 | 0 | 0 | 0 | 1 |
| ARR6 | 0 | 0 | 0 | 0 | 0 | 0 | 1 | 0 | 0 | 0 |
| ARR7 | 0 | 0 | 0 | 0 | 0 | 0 | 0 | 1 | 0 | 0 |
| ARR8 | 0 | 0 | 0 | 0 | 0 | 0 | 0 | 0 | 1 | 0 |
| ARR9 | 0 | 0 | 0 | 0 | 0 | 0 | 0 | 0 | 0 | 1 |

The fault signatures are not different from each other (I1 and I2) and not equal to zero, then the components I1 and I2 are not monitorable but R4, R5, R6, r2, I3, I4, C1 and C2 are monitorable.

$$\text{For } : [y_1 y_2 y_3 y_4 y_5 y_6 y_7 y_8 x_1 x_2] = [1111111110]$$

Table 2

Fault signature

| | I1 | I2 | R4 | R5 | R6 | r2 | I3 | I4 | C1 | C2 |
|------|----|----|----|----|----|----|----|----|----|----|
| ARR1 | 1 | 0 | 0 | 0 | 0 | 0 | 0 | 0 | 0 | 0 |
| ARR2 | 0 | 1 | 0 | 0 | 0 | 0 | 0 | 0 | 0 | 0 |
| ARR3 | 0 | 0 | 1 | 0 | 0 | 0 | 0 | 0 | 0 | 1 |
| ARR4 | 0 | 0 | 0 | 1 | 0 | 0 | 0 | 0 | 0 | 1 |
| ARR5 | 0 | 0 | 0 | 0 | 1 | 0 | 0 | 0 | 0 | 1 |
| ARR6 | 0 | 0 | 0 | 0 | 0 | 1 | 0 | 0 | 0 | 0 |
| ARR7 | 0 | 0 | 0 | 0 | 0 | 0 | 1 | 0 | 0 | 0 |
| ARR8 | 0 | 0 | 0 | 0 | 0 | 0 | 0 | 1 | 0 | 0 |
| ARR9 | 0 | 0 | 0 | 0 | 0 | 0 | 0 | 0 | 1 | 0 |

The fault signatures are different from each other and not equal to zero, then the components I1, I2, R4, R5, R6, r2, I3, I4, C1 and C2 are monitorable.

8. Simulation and interpretation

From SYMBOLS 2000, we have implanted the uncoupled Bond Graph model. For the faults detection of ultrasonic linear motor we use the precedent Analytical Redundancy Relations (ARRs). We create the faults on monitoring components with this software fault here is considered in the total absence or the deviation of the nominal value given out by the component to monitor.

The numeric values of components are not considered, only their presence or absences in the relation are taken in account with evaluation term the operators (+, -). It is the qualitative approach for Bond Graph monitoring.

8.1. Monitoring of I1 and the resistance R1

The diagram bloc of process is:

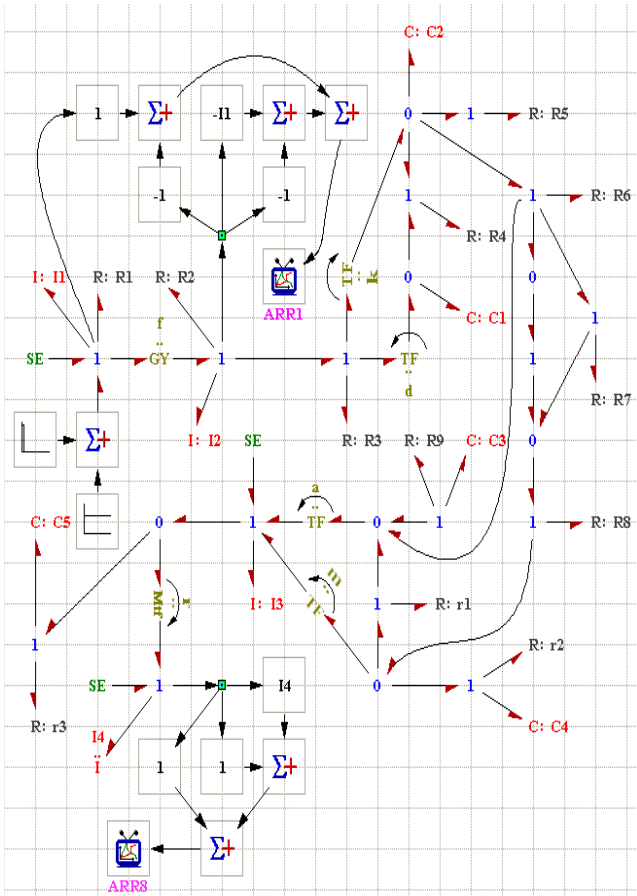


Fig.14. Diagram bloc

8.2. Monitoring of I2 and the resistance R2

By the same procedure we can monitored the components I2 and R2 the generated ARR's reaction is very fast see Fig. 16. The deviation of the relations ARR1, ARR4, ARR5, ARR6, ARR7, ARR8 and ARR9 in this time is normal (constant value). We see that residuals ARR2 is sensitive.

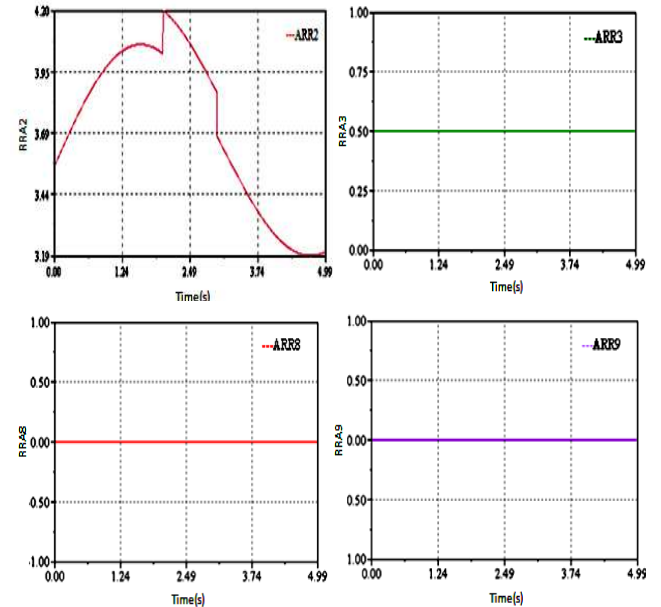


Fig.15. Sensitivity of detector Df2

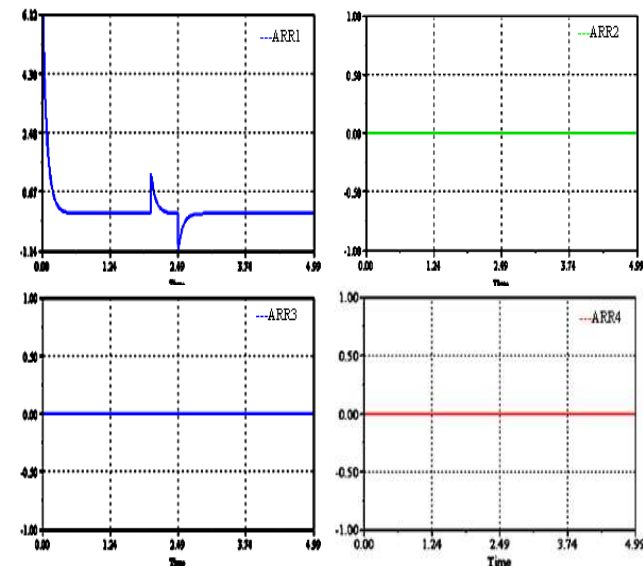


Fig.13. Sensitivity of detector Df1

The failures on I1 and R1 are characterized by the presence of the detector Df1 in the analytical redundancy relation ARR1. We note that the residual ARR1 is sensitive to the failures which affect I1 and R1, but residuals ARR2, ARR3, ARR4, ARR5, ARR6, ARR7, ARR8 and ARR9 are equals to zero.

8.3. Monitoring of C1

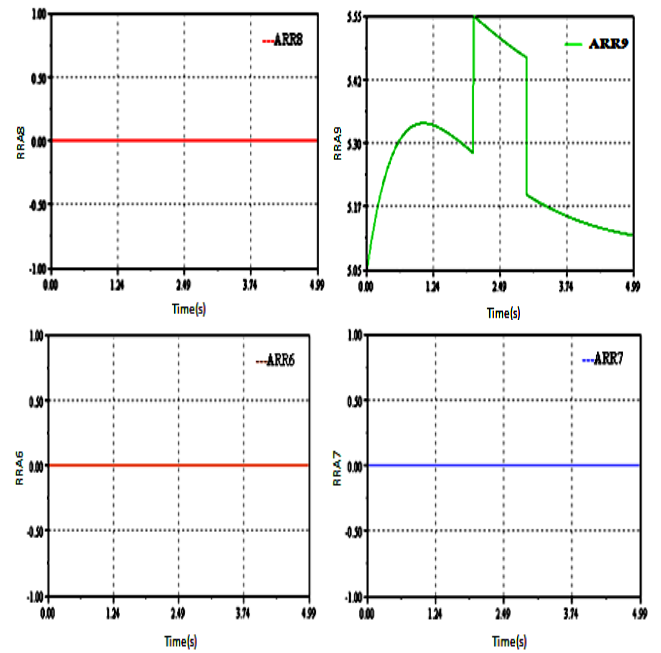


Fig.16. Sensitivity of detector Df1

The deviation of the relations ARR1, ARR2, ARR3, ARR4, ARR5, ARR6, ARR7 and ARR8 in this time is normal (constant value).

We see that residual ARR9 is sensitive due to the presence of De1 in this relation.

9. Conclusion

This work has presented piezomotors and more precisely, travelling wave ultrasonic annular motors. Its advantages and drawback have been explained. Piezomotors have specificities that are very interesting if they match application's needs: high torque/low speed, holding torque, silent operation, reactivity, high integration level. Because of the ultrasonic linear motor's complexity, precise analysis using analytic method is very difficult. Nevertheless, this modeling methodology has been presented in order to show that it is possible to model ultrasonic motors analytically. In the same way, the method of Bond Graph could be applied. Bond Graph is an explicit graphical tool for capturing the common energy structure of systems. In the vector form, it gives a concise description of complex systems. By this approach, a physical system can be represented by symbols and lines, identifying the power flow paths.

The method used illustrates the process principle working in that we use the structural junction equations for generating the analytical redundancy relations like failures indicators. The Bond Graph tool is the unified modeling method and it facilitates the functional and structural analysis of the complex systems. The multi-energy Bond Graph based approach used here for fault detection of the complex systems will be in perspective following by fault isolation and identification of eventual failure.

The tool Bond Graph and software SYMBOLS 2000 are proven powerful and convenient means for this project which included the modeling, the simulation and the analysis of the results. The results found here are proven interesting because the simulation of defects in quite precise moments were confirmed by the software of simulation starting from the sensitivity of the indicators installed.

Acknowledgments

The author would like to thank Belkacem Ould Bouamama PhD Polytech'Lille for useful discussions. Research reported in this manuscript was conducted at the automatic Laboratory of Setif University of Setif 19000 Algeria.

References

- [1] D. Jaume, M. Verge, Modélisation structurée des systèmes avec les Bond Graph". Edition technip, 2004.
- [2] V. Pifort, A. Preumont, finite element modeling of piezoelectric structures, Active Structures Laboratory ULB, 2001
- [3] H. Fukunaga, H. Kakehashi, H. Ogasawara and Y. Ohta, Effect of Dimension on Characteristics of Rosen-Type Piezoelectric Transformer, IEEE International Ultrasonics Symposium, 1998.
- [4] N. W. Hagood and J. Andrew, Modeling of a Piezoelectric Rotary Ultrasonic Motor, IEEE Transactions on Ultrasonic, Ferroelectrics, and Frequency Control, vol.42, n 2, pp.210-224, 1995.
- [5] S. H. Jeong, H. K. Lee, Y. J. Kim, H. H. Kim, and K. J. Lim, Vibration analysis of the stator in ultrasonic motor by FEM, Proceedings of the 5th International Conference on Properties and Applications of Dielectric Materials, pp.1091-1094, 1997.
- [6] A. Kawamura and N. Takeda, Linear Ultrasonic Piezoelectric Actuator, IEEE Trans. on Industry Applications, vol.27, n 1, pp. 23-26, 1991.
- [7] A.K. Samantaray, K. Medjaher, B. Ould Bouamama, M. Staroswiecki, G. Dauphin-Tanguy. Diagnostic bond graphs for online fault detection and isolation, Simulation Modelling Practice and Theory journal, page 237-262, July 2005.
- [8] W. Borutzky, Bond Graphs A Methodology for Modeling Multidisciplinary Dynamic Systems, volume FS-14 of Frontiers in Simulation, SCS Publishing House, Erlangen, San Diego, 2004, ISBN 3-936150-33-8.
- [9] B. D. Elmqvist, H., Olsson, H., Mattsson, S.E. Dymola for multi-engineering modeling and simulation. In: Proceedings of the Second International Modelica Conference, Oberpfaffenhofen, Germany, 55, pp. 1-8. 2002.
- [10] S. S. Rao, Mechanical vibrations, Addison-Wesley Publishing Company, USA, 1984.
- [11] T. Sashida, Ultrasonic Motors, Japanese Journal of Applied Physics, Vol .54, n°6, pp. 589-590, 1985.
- [12] S. Ueha and Y. Tomikawa, Ultrasonic Motors: Theory and Applications, Oxford University Press, 1993.
- [13] P. Helin, V. Sadaune, C. Druon and J. -B. Tritch, a Mechanical Model for Energy Transfer in Linear Ultrasonic Micromotors Using Lamb and Rayleigh Waves, IEEE/ASME Transactions on Mechatronics, vol.3, n 1, pp. 3-8, 1998.
- [14] T. Sashida and T. Kenjo, Introduction to Ultrasonic Motors, Oxford University Press, 1993.
- [15] C. Péclat, Conception et réalisation d'un micromoteur piézoélectrique, EPFL Thesis, n° 1434, 1995.
- [16] Khemliche M, B Ould Bouamama and H. Haffaf. Sensors placement for diagnosability on Bond Graph model, Sensors and actuators journal, page 92-98, volume n°4, March 2006